Radiometric Measurements of In-Cloud Temperature Fluctuations

BRUCE A. ALBRECHT

Department of Meteorology, The Pennsylvania State University, University Park 16802

STEPHEN K. COX AND WAYNE H. SCHUBERT

Department of Atmospheric Science, Colorado State University, Ft. Collins 80523

(Manuscript received 26 January 1979, in final form 12 May 1979)

ABSTRACT

The feasibility of measuring in-cloud temperature fluctuations with an infrared radiometer is demonstrated. The results obtained from aircraft measurements in a stratocumulus cloud deck indicate that a radiometer may easily resolve temperature variations within the cloud of less than 0.05°C provided that the cloud is sufficiently opaque. These radiometer measurements of temperature are combined with aircraft observations of vertical velocity to calculate a heat flux within the cloud deck. The heat flux derived using the radiometric observations shows excellent agreement with theoretical predictions of in-cloud heat flux. A similar heat flux calculation using the more conventional temperature transducer data was less by a factor of 5.

1. Introduction

The measurement of air temperature from an aircraft is relatively straightforward. A temperature sensitive device is placed in the airstream and the measured temperature is appropriately corrected for the heating of the air due to its deceleration in the vicinity of the sensor. This correction is in principal relatively straightforward since it depends only on the airspeed of the aircraft.

The aircraft measurement of air temperature within a cloud is more difficult, however, due to the complication of latent heat effects (Lenschow and Pennell, 1974). One method used to make in-cloud temperature measurements involves the use of a probe which is designed to prevent water droplets from impinging on the temperature element. Unfortunately, it is difficult to shield the element from droplets of all sizes. In heavy precipitation it is also difficult to ensure that moisture is not affecting the measurement.

In-cloud temperature measurements may also be obtained by measuring the wet-bulb temperature. From an aircraft, the temperature that is measured by this method is the wet-bulb temperature of the decelerated air in the vicinity of the sensor. In situations where aircraft speeds are not large the wet-bulb temperature and ambient temperature are nearly equal (Telford and Warner, 1962). This method of measurement, however, is limited to above freezing temperatures. Some method of ensuring that the sensor remains wet must also be used for the wet-bulb measurements. This consideration leads to a compromise between the sensor response time and the ability of the sensor to withstand the impact of large water drops.

A radiometric measurement of in-cloud temperatures may eliminate many of the complications encountered in the direct immersion of the thermometer in the airflow. Since the radiometer makes no direct contact with the airflow, it does not disturb the air volume being sampled. Furthermore, liquid water does not affect the physical operation of the radiometer.

The theoretical basis for the radiometric measurement of in-cloud temperatures is relatively straightforward. Since a cloud may be relatively opaque to infrared radiation, radiance measured from a given direction within the cloud is assumed to be proportional to a weighted average of the temperature in that direction. The radiance $N(\bar{\nu})$ measured by the radiometer as a function of emission from the matter within the conical field of view of the instrument is given as

$$N(\bar{\nu}) = \int_0^\infty P(\bar{\nu},T)\left(\frac{\partial \tau_\beta}{\partial l}\right)dl, \tag{1}$$

where $P(\bar{\nu},T)$ is the Planck relationship and $\tau(\bar{\nu})$ is the transmittance of the material in the path extending from the detector to a distance l from the plane of the detector. If we assume that the radiometer looks horizontally and that temperature does not vary in the horizontal, Eq. (1) becomes

$$N(\bar{\nu}) = P(\bar{\nu},T)\int_0^\infty \frac{\partial \tau_\beta}{\partial l}dl. \tag{2}$$

0021-8952/79/081066-06$05.50

But since

$$\int_0^\infty \frac{\partial \tau_{\tilde{\nu}}}{\partial l} dl \rightarrow 1.0 \qquad (3)$$

at 14.8 μm, the wavelength at which the measurements described in this paper are made, we have

$$N(\tilde{\nu}) = P(\tilde{\nu}, T). \qquad (4)$$

Hence the observed radiance may be related directly to temperature using Planck's law, $P(\nu,T)=C_1\nu^3/[\exp(C_2\nu/T)-1]$, where C_1 and C_2 are constants.

In rigorously deriving the relation given in Eq. (4), we assumed that T was invariant over the path l extending from 0 to ∞. In reality, it is neither practical nor necessary to extend this argument to the upper limit of infinity. Remembering that $\partial\tau_\nu/\partial l$ represents a weighting function applied to Planckian emission from a volume located a given distance l from the detector, we examine the results of a calculation of $\partial\tau/\partial l$ as a function of l. These calculations were based on the Mie calculations made by Tampieri and Tomasi (1976) for a wavelength of 15 μm and assume a liquid water content of 0.2 g m^{-3}. The drop size distribution assumed for this calculation was the stratocumulus distribution with a mode droplet radius of 4 μm given by Tampieri and Tomasi. The results shown in Fig. 1 indicate that within the cloud at a distance 10 m from the radiometer $\partial\tau/\partial l$ is 0.5 of the value at $l=0$, while at a distance of 33 m it is 0.1 of the $l=0$ value.

An estimate of $\partial\tau/\partial l$ for a clear-sky situation at a height of $\sim$500 m is also shown in Fig. 1. This curve was calculated from transmissivity data given by Smith.[1] In this case $\partial\tau/\partial l$ has a value of 0.1 at 200 m, a distance six times greater than for the in-cloud case. Consequently, in an optically thin cloud the effective sample volume becomes larger and the use of Eq. (4) rather than Eq. (1) becomes less acceptable; the possibility of errors introduced by aircraft roll also increases. The clear-air sample volume also varies with height since $\partial\tau/\partial l$ is density-dependent.

By measuring radiance from the aircraft along the horizontal plane of flight, the in-cloud temperature along the flight path may be determined. In the research described below, *in situ* aircraft measurements are used to evaluate the feasibility and limitations of radiometrically determining in-cloud temperatures.

2. Description of instrumentation

Radiometric temperature measurements within stratus off the coast of California were made from the NCAR Electra in June 1976. These measurements were made in conjunction with an experiment designed to measure various characteristics of stratocumulus convection. Details of this experiment are described by Wakefield and Schubert.[2] The radiometric temperature measurements were made using a Barnes PRT-6 infrared bolometer (manufactured by Barnes Engineering Company, Stamford, Connecticut) facing out the side of the aircraft. This radiometer was equipped with a band-pass filter with a maximum response at a wavelength of 14.8 μm. This wavelength is in a CO_2 absorption band and was chosen so that the measured radiance would be relatively insensitive to moisture fluctuations in situations where the cloud was optically thin. The radiometer was calibrated prior to the mission using a blackbody source to to obtain an explicit relationship between temperature and the voltage output of the PRT-6; during the flight a shutter whose temperature was monitored was periodically closed in front of the radiometer allowing in flight single-point calibrations.

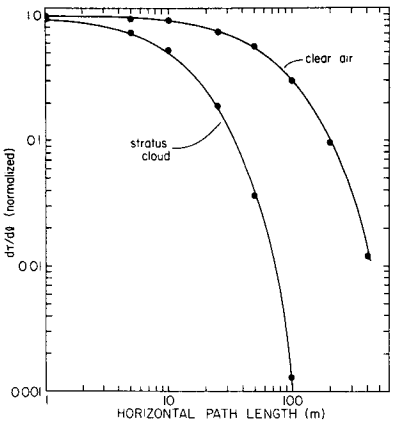

FIG. 1. Normalized values of $\partial\tau/\partial l$ for stratocumulus and clear sky conditions. Values are normalized by $\partial\tau/\partial l$ at $l=0$.

The radiometer employed in these measurements had a 2° field of view; therefore the temperature measured by the radiometer actually represents a weighted average of the temperature within a cone-shaped volume extending from the side of the aircraft. At a distance of 30 m from the aircraft, the base of the conical volume sampled is $\sim$1 m.

Simultaneous measurements of air temperature were also obtained from a Rosemount temperature probe (manufactured by Rosemount Engineering, Minneapolis, Minnesota). This probe is designed to prevent element breakage by the impingement of water droplets upon the resistance wire element used to make the temperature measurement. Although this probe is fairly effective in protecting the element from larger droplets, small droplets may result in wet-bulbing effects (Lenschow and Pennell, 1974).

[1] Smith, W. L., 1969: A polynomial representation of carbon dioxide and water vapor transmission. ESSA Tech. Rep. NESC 47, 20 pp.

[2] Wakefield, J. S., and W. H. Schubert, 1976: Design and execution of the marine stratocumulus experiment. Atmos. Sci. Pap. 256, Colorado State University, 74 pp. [NTIS PB 266-753].

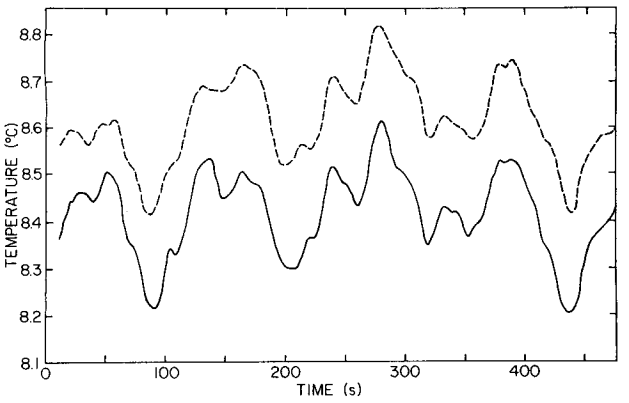

Fig. 2. Low-pass filtered PRT-6 (solid) and Rosemount (dashed) temperatures obtained from 19 June 1976 Electra flight, where $t=0$ is at 1419 GMT.

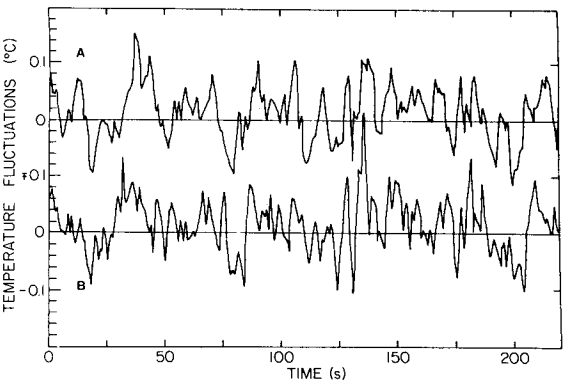

FIG. 3. High-pass filtered PRT-6 (curve A) and Rosemount (curve B) temperature fluctuations, where $t=0$ is at 1423 GMT.

If this effect is large it may be detected as a sudden decrease in the temperature trace.

3. Data analysis

The in-cloud temperature obtained from the infrared radiometer and the Rosemount probe were compared in order to evaluate the performance of the radiometer in measuring in-cloud temperatures. The data analyzed were collected from an 8.5 min in-cloud measurement at a constant pressure altitude of 965 mb. The PRT-6 data were prefiltered and recorded on magnetic tape at a rate of 20 Hz, while the Rosemount temperature was prefiltered and recorded at the rate of 1 Hz. To make these data compatible, the PRT-6 data was low-pass filtered using a normal curve smoothing function (Holloway, 1958). A visual inspection of the Rosemount temperature data showed no obvious degradation due to liquid water effects.

The PRT-6 and Rosemount temperature comparisons were made separately for high- and low-frequency fluctuations. The low-frequency data were obtained by filtering the data using a normal curve low-pass filter with a 20% response for fluctuations with a period of 14 s and an 80% response for fluctuations with a period of 42 s. The low-frequency PRT-6 and Rosemount temperature variations are shown in Fig. 2. Although there is 0.2°C offset between the absolute value of the two temperatures, the relative agreement between the temperature traces is excellent. Corresponding variations of less than 0.1°C are easily discernable.

High-frequency fluctuations were compared by calculating the power spectra for the PRT-6 and Rosemount temperatures. The data used in these calculations were obtained by high-pass filtering the 1 s data with a filter having a 20% response for fluctuations with a period of 100 s and an 80% response for fluctuations with a period of 37 s. The standard deviation of these filtered temperatures is 0.052°C for the PRT-6 temperatures and 0.045°C for the Rosemount temperatures. A segment of the high-pass filtered data is shown in Fig. 3. As was indicated previously, the low-frequency fluctuations compare favorably. However, for higher frequency fluctuations the relationship between the PRT-6 and Rosemount temperatures become less clear.

A spectral analysis of the high-pass filtered PRT-6 and Rosemount temperatures was made using the fast Fourier technique. The raw spectral estimates were averaged logarithmically into 30 spectral estimates with the lowest frequency estimate consisting of the average of three raw spectral modes and the highest frequency estimate consisting of the average of 15 raw spectral modes. The calculated spectra are shown in Fig. 4 and show good agreement at the lower frequencies, but noticeable departures appear between the spectra at 0.10 Hz. Although both spectra show peaks at 0.11 Hz, the variance associated with the PRT-6 fluctuations is significantly greater than that associated with the Rosemount. This feature may be noted in the time series shown in Fig. 3. Fluctuations having a period on the order of 10–12 s are

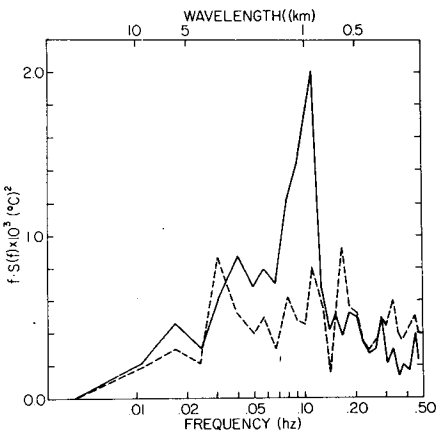

FIG. 4. Spectral estimates times frequency for PRT-6 (solid) and Rosemount (dashed) high-pass filtered temperatures.

easily discernable in the PRT-6 data. This is particularly true for the $t=100$ s to the $t=180$ s segment of the time series shown in Fig. 3. Although there is some indication of the 10–12 s fluctuations in the Rosemount data, they are not as clearly defined as those in the PRT-6 temperatures. Both sensors show relatively small amounts of variance at frequencies >0.15 Hz.

Although the differences in the high-frequency fluctuations discussed above are on the order of ~0.05°C, they can result in significant differences in the heat flux calculated with these temperature fluctuations. A heat flux ($\rho c_p \overline{w'T'}$) calculated for the data segment described above is 4.1 W m^{-2} using the PRT-6 temperatures and 0.9 W m^{-2} for the Rosemount temperatures. These fluxes were calculated using a constant air density ρ of 1.2 kg m^{-3}. The cospectra $C(f)$ of vertical velocity w and the Rosemount and PRT-6 temperatures are shown in Fig. 5. The area under these curves represents $\overline{w'T'}$. The positive nature of the flux calculated with the PRT-6 is clearly evident. A positive correlation between vertical velocity and temperature may be noted from 0.07–0.12 Hz. Although the Rosemount temperature and vertical velocity are positively correlated at 0.11 Hz, they are negatively correlated at 0.10 Hz.

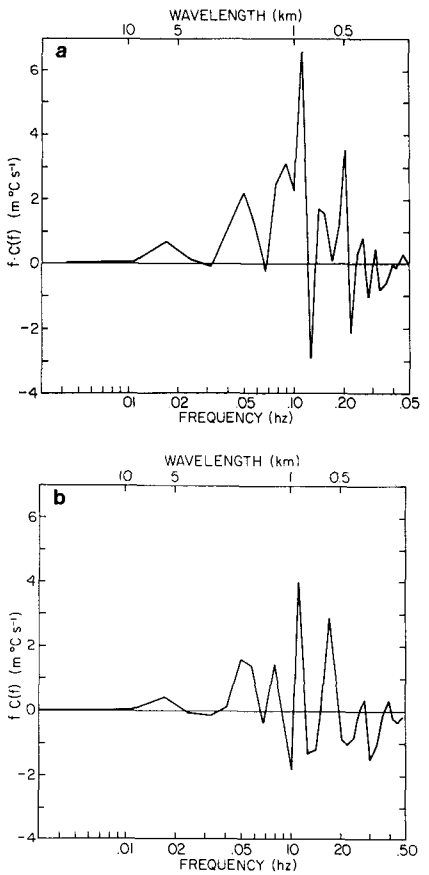

FIG. 5. Cospectral estimates times frequency for (a) vertical velocity and PRT-6 temperature and (b) vertical velocity and Rosemount temperature.

TABLE 1. Correlation coefficient for T_E and droplet concentrations and the percent of liquid water at a given size range as determined from droplet concentrations.

Radius (μm)	Correlation coefficient	Percent of liquid water
1.5– 4.5	0.03	0.6
4.5– 7.5	−0.21	24.6
7.5–10.5	−0.18	63.7
10.5–13.5	0.05	4.6
13.5–16.5	0.01	4.2
16.5–19.5	0.00	1.1
19.5–22.5	0.06	1.1

It is significant to note that the theoretical estimates of the virtual heat flux within a stratocumulus cloud layer given by Schubert *et al.* (1979) is ~5 W m^{-2} for a sea surface temperature of 13°C and a divergence of 5×10^{-6} s^{-1}. The sea surface temperature estimated from a downward looking radiometer mounted on the Electra indicate a sea surface temperature of ~10°C for the measurements discussed here. Consequently, we would expect the heat flux to be slightly less than the virtual heat flux over water having a temperature of 13°C. The heat flux calculated with the Rosemount temperatures is significantly less than that given by the theoretical calculation, while that given by the PRT-6 temperatures is of the same magnitude. Since the response times of the PRT-6 and the Rosemount are both less than 1 s, the differences in the fluxes are not due to instrument lags.

The discrepancies between the Rosemount and PRT-6 temperatures may be due to wetting of the Rosemount sensor. Although the Rosemount is designed to prevent larger water droplets from impinging on the resistance wire elements, smaller droplets may not be effectively filtered out. To test this hypothesis, a time series was constructed of the difference between the Rosemount and PRT-6 temperatures. This difference will be defined as $T_E = T_R - T_P$, where T_R is the Rosemount temperature and T_P the PRT-6 temperature. A high-pass filtered time series of water droplet concentrations for different droplet sizes was obtained from a Particle Measuring Systems (PMS) Spectrometer Probe (manufactured by Particle Measuring Systems, Boulder, Colorado). Correlation coefficients for T_E and droplet concentrations of various droplet sizes are shown in Table 1. The interesting feature of these results is the negative correlation between T_E and the concentration of droplets with radii in the 4.5–10.5 μm range. This negative correlation is what one would expect if smaller droplets result in a wetting of the Rosemount sensor. In this situation an increase in droplet concentration would result in a decrease in

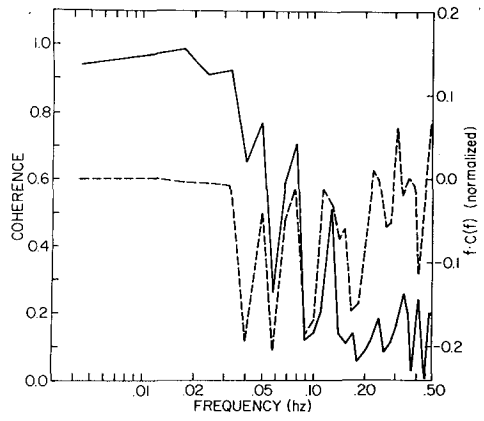

FIG. 6. Coherence between PRT-6 and Rosemount high-pass filtered temperatures (solid) and normalized cospectra for T_E and PMS droplet concentrations in the 4.5–7.5 μm radius range (dashed).

the Rosemount temperature. Note that although one would also expect a negative correlation for droplets in the 1.5–4.5 μm range, less than 1% of the liquid water is associated with droplets of this size.

Cospectral estimates were calculated for T_E and the PMS droplet concentrations. The normalized cospectrum for T_E and droplets in the 4.5–7.5 μm range is shown in Fig. 6. This curve represents the relative contribution of fluctuations at various frequencies to the negative correlation between T_E and the droplet concentrations shown in Table 1. It is interesting to note that this contribution is negative at nearly all frequencies. The largest contributions to the negative correlation are found at frequencies of 0.4, 0.06 and 0.08 Hz. The coherence calculated for the Rosemount and PRT-6 temperatures is also shown in Fig. 6 and has relative minimums at 0.4, 0.06 and 0.08 Hz.

Errors in the PRT-6 temperature may also account for at least some of the differences between the Rosemount and PRT-6 temperatures. For example, as the liquid water decreases the volume effectively sampled by the PRT-6 increases. However, it is not obvious why this increase in volume would systematically result in the decrease in PRT-6 temperatures that would be needed to explain the correlations noted in Table 1 and Fig. 5. The differences between the Rosemount and PRT-6 temperatures may also be due to the fact that the PRT-6 temperature may be more strongly weighted toward the cloud droplet temperature than the actual air temperature. In an updraft one would expect the droplet temperatures to be slightly warmer than the environment. For the updrafts associated with stratocumulus convection one would not expect supersaturations to significantly exceed 0.1% (Fletcher, 1962). Hence, temperature differences between the droplets and the air should generally be less than 0.02°C. The fluctuations shown in Fig. 3 are on the order of 0.08°C which is significantly larger than the droplet–air temperature differences. This effect could, however, result in a slight overestimate of the heat flux. For radiometric temperature measurements made in clouds having very strong updrafts or downdrafts, the droplet–air temperature difference may be significant.

4. Conclusions

The results given above indicate the feasibility of using an aircraft-mounted infrared radiometer to measure in-cloud temperatures. Temperature in a stratocumulus deck were obtained using an infrared radiometer and an immersion type temperature probe. Low-frequency fluctuations in the two measurements are nearly identical. The agreement is not as good, however, for fluctuations corresponding to a horizontal scale less than 2 km. Although these differences are relatively small, an in-cloud heat flux calculated with radiometer temperatures is 4.1 W m^{-2}, while that calculated using data from the conventional Rosemount temperature probe is 0.9 W m^{-2}. A plausible explanation for these differences appears to be the wetting of the Rosemount sensor. This interpretation is consistent with the negative correlation calculated between differences in the Rosemount and radiometer temperatures and the concentrations of droplets having radii from 4.5–10.5 μm. This wetting effect would be greatest in the updrafts and may account for the smaller heat flux obtained with the Rosemount temperatures. While radiometer temperatures may result in a slight overestimate of the heat flux since water droplets in an updraft may be slightly warmer than the air temperature, the heat flux calculated using the radiometric observations shows significantly better agreement with theoretical estimates of the in-cloud heat flux than those obtained using the more conventional temperature transducer.

Although the accuracy of the radiometric measurements may be limited in cases where cloud updrafts and downdrafts are very strong, fluctuations of less than 0.05°C are resolvable in an optically thick cloud with moderate supersaturation or subsaturations. The radiometric method of measurement has a distinct advantage over immersion thermometer techniques since the radiometer in no way disturbs the air being sampled and liquid water has no direct effect on the physical operation of the radiometer.

Acknowledgments. We gratefully acknowledge the cooperation and support of the NCAR Research Aviation Facility during the field phase of this research. Drs. D. Lenschow and D. Lilly read this manuscript and made useful comments. This research was funded by the Global Atmospheric Research Program, Division of Atmospheric Sciences, National Science Foundation and the GATE Project Office,

National Oceanic and Atmospheric Administration under Grants ATM 77-15369, ATM 78-05743, ATM 78-08125 and ATM 78-09715.

REFERENCES

Fletcher, N. H., 1962: *The Physics of Rainclouds*. Cambridge University Press, 285 pp.

Holloway, J. L., Jr., 1958: Smoothing and filtering of time series and space fields. *Advances in Geophysics*, Vol. 4, Academic Press, 351–399.

Lenschow, D. H., and W. T. Pennell, 1974: On measurement of in-cloud and wet-bulb temperatures from an aircraft. *Mon. Wea. Rev.*, **102**, 447–454.

Schubert, W. H., J. S. Wakefield, E. J. Steiner and S. K. Cox, 1979: Marine stratocumulus convection, Part I: Governing equations and horizontally homogenous solutions. *J. Atmos. Sci.*, **36**, 1286–1307.

Tampieri, F., and C. Tomasi, 1976: Size distribution models of fog and cloud droplets and their volume extinction coefficients at visible and infrared wavelengths. *Pure Appl. Geophys.*, **114**, 571–586.

Telford, J., and J. Warner, 1962: On the measurement from an aircraft of buoyancy and vertical air velocity in cloud. *J. Atmos. Sci.*, **19**, 415–423.